Journal of Biomolecular NMR, **18:** 261–268, 2000.
KLUWER/ESCOM

Transverse relaxation optimized 3D and 4D ^{15}N/^{15}N separated NOESY experiments of ^{15}N labeled proteins

Youlin Xia, KongHung Sze & Guang Zhu*
Department of Biochemistry, The Hong Kong University of Science and Technology, Clear Water Bay, Kowloon, Hong Kong, SAR

Received 21 June 2000; Accepted 6 September 2000

Key words: HSQC, ^{15}N labeled protein, NOESY, TROSY

Abstract

NMR studies of protein structures require knowledge of spectral assignments through correlation spectroscopy and the measurement of dipolar interactions by NOESY-type experiments. In order to obtain NOEs for protons with degenerate chemical shifts, which is particularly common for large proteins with significant helical content, 3D and 4D ^{15}N/^{15}N separated NOESY experiments (HSQC-NOESY-HSQC) are essential for NMR studies of these proteins. TROSY sections could replace the latter or both HSQC parts of the 3D and 4D ^{15}N/^{15}N separated HSQC-NOESY-HSQC pulse sequences to enhance signal sensitivity and improve resolution. For a 1.0 mM, 100% ^{15}N and 70% ^{2}H-labeled Trichosanthin sample (∼27 kDa) at 5 °C it is found that sensitivity enhancements could only be obtained when TROSY sections replace the latter HSQC parts of 3D and 4D ^{15}N/^{15}N separated HSQC-NOESY-HSQC pulse sequences. The sensitivities of 3D and 4D HSQC-NOESY-TROSY experiments are enhanced by 62% and 8% at 5 °C, respectively, compared to their corresponding 3D and 4D HSQC-NOESY-HSQC experiments. Furthermore, the corresponding linewidths are, on average, decreased by 20% and 18% Hz in the H_N and N2 dimensions, respectively. This enhancement of sensitivity depends on the molecular mass of the sample used and the lengths of the evolution times in the indirectly and directly detected dimensions.

Introduction

The recent development of Transverse Relaxation Optimized Spectroscopy (TROSY) techniques has made it possible to study proteins larger than 30 kDa (Pervushin et al., 1997). Several TROSY-based experiments with uniformly ^{13}C, ^{15}N and ^{2}H-labelled proteins, designed for spectral assignment, have been published (Pervushin et al., 1998; Salzmann et al., 1998, 1999a,b; Weigelt, 1998; Zhu et al., 1998; Yang and Kay, 1999). To obtain structural information from large ^{15}N labeled proteins, and to alleviate the problem of spectral overlap caused by the great increase in the number of proton signals, 3D NOESY-TROSY experiments have been proposed to measure the dipole–dipole interaction among protons (Pervushin et al., 1999; Zhu et al., 1999a,b). Nevertheless, the 3D NOESY-TROSY experiments may still be insufficient to provide unambiguous measurements of NOEs among the overlapping proton signals. This is particularly acute in proteins with a high level of helical content. To further alleviate the spectral overlap problem, we describe here four NOESY experiments, namely, 3D and 4D ^{15}N/^{15}N separated HSQC-NOESY-TROSY and TROSY-NOESY-TROSY, which are analogous to the HMQC-NOESY-HMQC or HSQC-NOESY-HSQC experiments (Frenkiel et al., 1990; Ikura et al., 1990; Kay et al., 1990; Zuiderweg et al., 1991; Muhandiram et al., 1993; Vuister et al., 1993). Perdeuteration of the protein sample not only increases the amide proton T_2, and the TROSY effect dramatically, but also reduces the occurrence of spin diffusion, permitting detection of NOEs among protons separated more than 5 Å by using longer NOE

*To whom correspondence should be addressed. E-mail: gzhu@ust.hk

mixing times (Torchia et al., 1988; Venters et al., 1995). Hence, the TROSY-based 3D and 4D ^{15}N/^{15}N separated NOESY experiments could be very useful for structure determination of large proteins.

It was reported that up to threefold sensitivity gains were obtained by using TROSY-type triple resonance experiments with a ^{15}N, ^{13}C and ^{2}H isotopically labeled 23 kDa protein when compared with the corresponding conventional implementations (Salzmann et al., 1998, 1999a,b; Yang and Kay, 1999). To obtain similar results in ^{15}N/^{15}N separated NOESY experiments, the TROSY section could replace the latter or both HSQC parts of the HSQC-NOESY-HSQC pulse sequence to form the 3D and 4D ^{15}N/^{15}N separated HSQC-NOESY-TROSY and TROSY-NOESY-TROSY experiments, respectively. The differences in the sensitivity of the four experiments are examined in detail in this work.

Theory

The 3D and 4D ^{15}N/^{15}N separated HSQC-NOESY-TROSY pulse sequences are shown in Figures 1A and 1B, respectively. In these two pulse sequences, the TROSY sequences replace the latter gradient and sensitivity enhanced HSQC sections in the 3D and 4D ^{15}N/^{15}N separated HSQC-NOESY-HSQC pulse sequences. The 3D and 4D ^{15}N/^{15}N separated TROSY-NOESY-TROSY pulse sequences are shown in Figures 1C and 1D, respectively. In the 3D ^{15}N/^{15}N separated TROSY-NOESY-TROSY pulse sequence (Figure 1C), the slowly relaxing components in the t_1 dimension are selected with the S^{3}E (Spin State Selective Excitation) scheme (Meissner et al., 1997; Sørensen et al., 1997; Pervushin et al., 1998; Zhu et al., 1999b). In Figures 1C and 1D, the idea of total TROSY is realized; that is, the slowly relaxing components are selected in all dimensions. In general, 3D experiments could be carried out with the corresponding 4D versions of the HSQC-NOESY-TROSY (Figure 1B) and TROSY-NOESY-TROSY (Figure 1D) pulse sequences with t_2 being set to zero. However, *x*- and *y*-components of ^{15}N coherence cannot be transferred simultaneously to the detected ^{1}H for 3D ^{15}N/^{15}N separated NOESY experiments, and only one component needs to be transferred to ^{1}H with an INEPT. By doing so, 5.4 ms for an INEPT is saved in the 3D HSQC-NOESY-TROSY (Figure 1A) experiment compared with a 3D version ($t_2 = 0$) of the 4D HSQC-NOESY-TROSY (Figure 1B) experiment. Similarly, for the 3D TROSY-NOESY-TROSY pulse sequence, about 2.7 ms for half an INEPT is saved compared with a 3D version ($t_2 = 0$) of 4D TROSY-NOESY-TROSY (Figure 1D). Note that the sensitivity enhancement scheme of PEP (Preservation of Equivalent Path) (Palmer et al., 1991; Kay et al., 1992) is still effective in Figure 1B. The use of PEP enhances sensitivity by 31% on average for 124 well-isolated peaks from 2D HSQC and TROSY spectra for the Trichosanthin sample at 5 °C in the present study.

For all four pulse sequences, water magnetization is retained along the +z axis direction before detection, and small bipolar gradients are used to suppress the effect of water radiation damping. The carrier of proton radio frequency in the F_2 dimension of 4D experiments is positioned at 7.7 ppm, so that the proton spectral width can be reduced to 2900 Hz to enhance digital resolution in this dimension.

Four transients are acquired in the two 3D experiments, as described in the captions of Figures 1A and 1C. The detectable signals for the 3D HSQC-NOESY-TROSY experiment (Figure 1A) are:

$$S_{11} \propto u \cos(\omega_S t_1) \exp(+i\omega_{S'\alpha} t_2) \exp\left(i\omega_{I'\beta} t_3\right)$$
$$S_{12} \propto u \cos(\omega_S t_1) \exp(-i\omega_{S'\alpha} t_2) \exp\left(i\omega_{I'\beta} t_3\right)$$
$$S_{21} \propto u \sin(\omega_S t_1) \exp(+i\omega_{S'\alpha} t_2) \exp\left(i\omega_{I'\beta} t_3\right)$$
$$S_{22} \propto u \sin(\omega_S t_1) \exp(-i\omega_{S'\alpha} t_2) \exp\left(i\omega_{I'\beta} t_3\right)$$

where u is the magnitude of ^{1}H steady state magnetization (Pervushin et al., 1998); S' and I' are nuclei spins of the ^{15}N-^{1}H moiety connected to S and I through NOE contact; ω_X is the Larmor frequency of nucleus X, $\omega_{S'\alpha} = \omega_{S'} + \pi J$, $\omega_{I'\beta} = \omega_{I'} - \pi J$; J is the coupling constant between nuclei I and S, or I' and S'. The corresponding detectable signals of the 3D TROSY-NOESY-TROSY experiment (Figure 1C) are identical to the above form, except that u and ω_S are replaced with $(u+\nu)$ and $\omega_{S\alpha}$ ($\omega_{S\alpha} = \omega_S + \pi J$), respectively, where ν is the magnitude of ^{15}N steady state magnetization. 3D NMR spectra can be obtained by using the Rance–Kay processing method (Palmer et al., 1991; Kay et al., 1992).

In the two 4D experiments, eight transients are acquired through changing phases and gradients in the manner described in the captions of Figures 1B and 1D. The detectable signals for the 4D HSQC-NOESY-

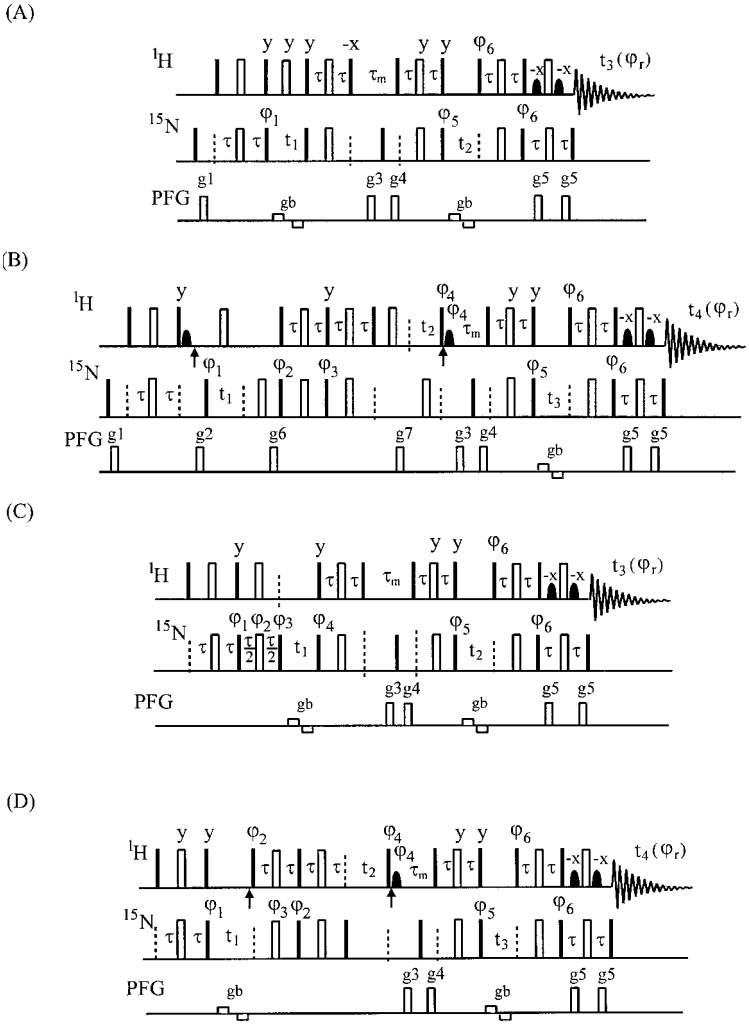

Figure 1. HSQC-NOESY-TROSY pulse sequences: (A) 3D version and (B) 4D version; TROSY-NOESY-TROSY pulse sequences: (C) 3D version and (D) 4D version. Filled bars and open bars represent 90° and 180° pulses, respectively. Filled shaped pulses are 1.1 ms sinc-modulated rectangular 90° pulses to selectively excite the water resonance. The experimental recovery delay is 1 s. $\tau = 2.5$ ms, $\tau_m = 100$ ms. The durations and strengths of the gradients are g1 = (1.0 ms, 25 G/cm); g2 = (0.4 ms, 15 G/cm); g3 = (90 ms, 1 G/cm); g4 = (4 ms, 1 G/cm); g5 = (0.5 ms, 20 G/cm); g6 = (1 ms, 25 G/cm); g7 = (0.1 ms, 0.967 × 25 G/cm); gb are smaller bipolar gradients to suppress the effect of water radiation damping; the paired gradients can also be applied on both sides of all paired 180° pulses to remove the imperfections of these pulses. Default phases are x. For the two 4D experiments, the carrier of proton between the two arrows in (B) and (D) is positioned at 7.7 ppm and elsewhere returned to 4.7 ppm. For 3D experiments, 4 transients, $S_{\text{phase1,phase2}}$ (phase1=1,2; phase2=1,2 as explained in the following), were recorded; for 4D experiments, 8 transients, $S_{\text{phase1,phase2,phase3}}$ (phase1=1,2; phase2=1,2; phase3=1,2), were recorded. (A): φ_1=(x,x,−x,−x); φ_5=(y,x,y,x,−y,−x,−y,−x); φ_6=(y); φ_r=(x,−y,−x,y,−x,y,x,−y). If phase1=2, $\varphi_1 = \varphi_1 + 90°$, else φ_1 is not varied; if phase2=2, $\varphi_6 = \varphi_6 + 180$ °C and reversing the sign of the even number step phases of φ_r, else φ_6 and φ_r are not varied. Axial peaks were removed by setting ($\varphi_1 + 180°$, $\varphi_r + 180°$), and ($\varphi_5 + 180°$, $\varphi_r + 180°$) for every second t_1 and t_2 increment, respectively. (B): φ_1=(y,−y); φ_2=(−x); φ_3=(y); φ_4=(y); φ_5=(y,y,x,x); φ_6=(y); φ_r=(x,−x,−y,y). If phase1=2, $\varphi_4 = \varphi_4 - 90°$, else φ_4 is not varied; if phase2=2, $\varphi_2 = \varphi_2 + 180°$ and the sign of g6 is inverted, else φ_2 and g6 are not varied; if phase3=2, $\varphi_6 = \varphi_6 + 180°$ and reversing the sign of the third and fourth step phases of φ_r, else φ_6 and φ_r are not varied. Axial peaks were removed by setting ($\varphi_1 + 180°$, $\varphi_r + 180°$), ($\varphi_2 + 180°$, $\varphi_3 + 180°$, $\varphi_r + 180°$), and ($\varphi_5 + 180°$, $\varphi_r + 180°$) for every second t_1, t_2, and t_3 increment, respectively. (C): φ_1=(4(x),4(−x)) + 45°; φ_2=(x); φ_3=(y); φ_4=(x); φ_5=(y,x,−y,−x); φ_6=(y); φ_r=(x,−y,−x,y,−x,y,x,−y). If phase1=2, $\varphi_4 = \varphi_4 - 90°$, else φ_4 is not varied; if phase2=2, $\varphi_6 = \varphi_6 + 180°$ and reversing the sign of the even number step phases of φ_r, else φ_6 and φ_r are not varied. Axial peaks were removed by setting ($\varphi_1 + 180°$, $\varphi_2 + 180°$, $\varphi_3 + 180°$, $\varphi_r + 180°$), and ($\varphi_5 + 180°$, $\varphi_r + 180°$) for every second t_1 and t_2 increment, respectively. (D): φ_1=(y,x,−y,−x); φ_2=(y); φ_3=(x); φ_4=(x,−y); φ_5=4(y),4(x); φ_6=(y); φ_r=(x,x,−x,−x,−y,−y,y,y). If phase1=2, $\varphi_4 = \varphi_4 - 90°$, else φ_4 is not varied; if phase2=2, $\varphi_2 = \varphi_2 + 180°$ and reversing the sign of the second step phases of φ_4, else φ_2 and φ_4 are not varied; if phase3=2, $\varphi_6 = \varphi_6 + 180°$ and reversing the sign of the last four step phases of φ_r, else φ_6 and φ_r are not varied. Axial peaks were removed by setting ($\varphi_1 + 180°$, $\varphi_r + 180°$), ($\varphi_3 + 90°$, $\varphi_r + 180°$), and ($\varphi_5 + 180°$, $\varphi_r + 180°$) for every second t_1, t_2, and t_3 increment, respectively.

TROSY experiment (Figure 1B) are:

$$S_{111} \propto u \cos(\omega_S t_1 + \omega_I t_2) \exp\left(+i\omega_{S'\alpha} t_3\right) \exp\left(i\omega_{I'\beta} t_4\right)$$

$$S_{112} \propto u \cos(\omega_S t_1 + \omega_I t_2) \exp\left(-i\omega_{S'\alpha} t_3\right) \exp\left(i\omega_{I'\beta} t_4\right)$$

$$S_{121} \propto u \cos(-\omega_S t_1 + \omega_I t_2) \exp\left(+i\omega_{S'\alpha} t_3\right) \exp\left(i\omega_{I'\beta} t_4\right)$$

$$S_{122} \propto u \cos(-\omega_S t_1 + \omega_I t_2) \exp\left(-i\omega_{S'\alpha} t_3\right) \exp\left(i\omega_{I'\beta} t_4\right)$$

$$S_{211} \propto u \sin(\omega_S t_1 + \omega_I t_2) \exp\left(+i\omega_{S'\alpha} t_3\right) \exp\left(i\omega_{I'\beta} t_4\right)$$

$$S_{212} \propto u \sin(\omega_S t_1 + \omega_I t_2) \exp\left(-i\omega_{S'\alpha} t_3\right) \exp\left(i\omega_{I'\beta} t_4\right)$$

$$S_{221} \propto u \sin(-\omega_S t_1 + \omega_I t_2) \exp\left(+i\omega_{S'\alpha} t_3\right) \exp\left(i\omega_{I'\beta} t_4\right)$$

$$S_{222} \propto u \sin(-\omega_S t_1 + \omega_I t_2) \exp\left(-i\omega_{S'\alpha} t_3\right) \exp\left(i\omega_{I'\beta} t_4\right)$$

The quadrature components, $S'_{ijk}(i, j, k = 1, 2)$, can be obtained through the following combinations:

$$S_{111} + S_{112} + S_{121} + S_{122}$$
$$\propto 4u \cos(\omega_S t_1) \cos(\omega_I t_2) \cos(\omega_{S'\alpha} t_3) \exp(i\omega_{I'\beta} t_4)$$
$$\longrightarrow S'_{111}$$

$$S_{111} - S_{112} + S_{121} - S_{122}$$
$$\propto i4u \cos(\omega_S t_1) \cos(\omega_I t_2) \sin(\omega_{S'\alpha} t_3) \exp(i\omega_{I'\beta} t_4)$$
$$\xrightarrow{90^\circ} S'_{112}$$

$$S_{211} + S_{212} + S_{221} + S_{222}$$
$$\propto 4u \cos(\omega_S t_1) \sin(\omega_I t_2) \cos(\omega_{S'\alpha} t_3) \exp(i\omega_{I'\beta} t_4)$$
$$\longrightarrow S'_{121}$$

$$S_{211} - S_{212} + S_{221} - S_{222}$$
$$\propto i4u \cos(\omega_S t_1) \sin(\omega_I t_2) \sin(\omega_{S'\alpha} t_3) \exp(i\omega_{I'\beta} t_4)$$
$$\xrightarrow{90^\circ} S'_{122}$$

$$S_{211} + S_{212} - S_{221} - S_{222}$$
$$\propto 4u \sin(\omega_S t_1) \cos(\omega_I t_2) \cos(\omega_{S'\alpha} t_3) \exp(i\omega_{I'\beta} t_4)$$
$$\longrightarrow S'_{211}$$

$$S_{211} - S_{212} - S_{221} + S_{222}$$
$$\propto i4u \sin(\omega_S t_1) \cos(\omega_I t_2) \sin(\omega_{S'\alpha} t_3) \exp(i\omega_{I'\beta} t_4)$$
$$\xrightarrow{90^\circ} S'_{212}$$

$$-S_{111} - S_{112} + S_{121} + S_{122}$$
$$\propto 4u \sin(\omega_S t_1) \sin(\omega_I t_2) \cos(\omega_{S'\alpha} t_3) \exp(i\omega_{I'\beta} t_4)$$
$$\longrightarrow S'_{221}$$

$$-S_{111} + S_{112} + S_{121} - S_{122}$$
$$\propto i4u \sin(\omega_S t_1) \sin(\omega_I t_2) \sin(\omega_{S'\alpha} t_3) \exp(i\omega_{I'\beta} t_4)$$
$$\xrightarrow{90^\circ} S'_{222}$$

where 90° in the above equations indicates a 90° phase shift. A pure 4D absorption HSQC-NOESY-TROSY spectrum can be achieved by Fourier transformation of the FIDs made up of the quadrature components, S'_{ijk}, described above.

The detectable signals for the 4D TROSY-NOESY-TROSY experiment (Figure 1D) are identical to the above form, except that the u, ω_S and ω_I are replaced with (u+v), $\omega_{S\alpha}$ and $\omega_{I\beta}$ ($\omega_{I\beta} = \omega_I - \pi J$), respectively.

Experimental and results

To demonstrate the proposed 3D and 4D ^{15}N/^{15}N separated NOESY experiments, we applied them to a uniformly 100% ^{15}N and 70% ^{2}H-labelled Trichosanthin sample (~27 kDa, 1.0 mM in 20 mM Na_2HPO_4, pH 6.8, 95% H_2O/5% D_2O) on a Varian Inova 750 MHz NMR spectrometer at 5 °C and 25 °C. Except where indicated, spectra were recorded at 5 °C. All data processing was performed using the NMRPipe software package (Delaglio et al., 1995).

The TROSY effect is significant in constant time type experiments, such as the [^{15}N,^{1}H]-TROSY-HNCA and [^{15}N,^{1}H]-TROSY-HNCO experiments (Salzmann et al., 1998), but it is less pronounced in non-constant time type experiments. The effectiveness of TROSY depends on the lengths of evolution periods in the indirectly and directly detected dimensions in these experiments, which in turn depends on the number of data points acquired with given spectral widths. Two 2D spectra ($t_1 = 0$) of 3D HSQC-NOESY-TROSY and its corresponding 3D HSQC-NOESY-HSQC experiment with mixing time $\tau_m = 100$ ms were recorded to compare their sensitivities. The data matrices in the time domain for the two 2D spectra were composed of $216^* \times 2048^*$ points, with spectral widths of 1825×10500 Hz. The processed 2D spectra were composed of 512×4098 points. For the 118 well-isolated peaks examined, the signal sensitivities are enhanced by −10% to 267%. On average, the sensitivity of the former experiment is enhanced by 102% compared to that of the latter experiment. If only $108^* \times 2048^*$, $54^* \times 2048^*$, and $32^* \times 2048^*$ points of the two data matrices in the time domain are taken to be processed, the sensitivity is, on average, enhanced by 62%, 35%, and 20%, respectively. Two 2D experiments were recorded at 25 °C with $108^* \times 2048^*$ data points, where the sensitivity is enhanced by 11%. These results indicate that the sensitivity enhancement

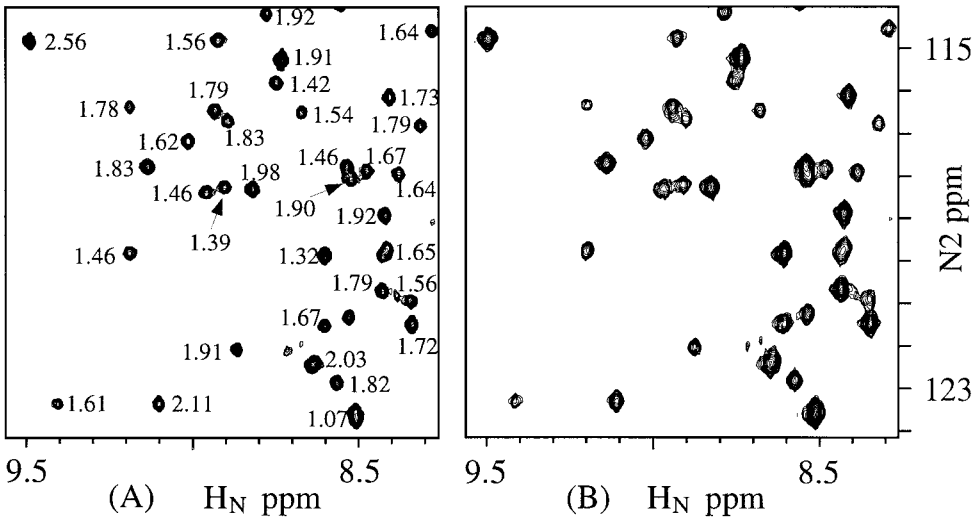

Figure 2. Small regions of 2D spectra ($t_2 = 0$) of $^{15}N/^{15}N$ separated 3D HSQC-NOESY-TROSY (A) and its corresponding 3D HSQC-NOESY-HSQC (B) experiments of a uniformly 100% ^{15}N and 70% ^{2}H-labeled Trichosanthin sample at 5 °C on a Varian Inova 750 MHz NMR spectrometer. The chemical shifts of the N2 and H_N dimensions in Figure 2A were shifted by 45 Hz compared with those in Figure 2B. The numbers beside the peaks of Figure 2A are the intensity ratios of peaks in Figure 2A and their corresponding peaks in Figure 2B. Figure 2A and Figure 2B have identical lowest contours and a contour factor of 1.2.

due to the TROSY effect depends on the lengths of the evolution periods in the indirectly and directly detected dimensions. The two 2D spectra ($t_1 = 0$) of 3D HSQC-NOESY-TROSY and its corresponding 3D HSQC-NOESY-HSQC experiments, composed with $108^* \times 2048^*$ points in the time domain, are shown in Figures 2A and 2B, respectively. The numbers beside the peaks of Figure 2A are the ratios of peak intensities in Figure 2A over their corresponding peak intensities in Figure 2B. For the 118 well-isolated peaks examined, the signal sensitivities are enhanced by -18% to 178%. On average, a sensitivity enhancement of 62% is obtained. It is shown that the peaks in Figure 2A are much sharper than those in Figure 2B. The linewidths in the H_N (F_3) and N2 (F_2) dimensions are reduced by 3–55% and 2–45%, respectively. On average, the linewidths are decreased by 20% and 18% in the H_N and N2 dimensions, respectively.

Two 3D $^{15}N/^{15}N$ separated HSQC-NOESY-TROSY and HSQC-NOESY-HSQC spectra were acquired. Data matrices in the time domain were composed of $54^* \times 108^* \times 2048^*$ points, with a spectral width of $1825 \times 1825 \times 10500$ Hz. The number of scans for each transient was 8. Cosine-bell window functions were used to obtain the 3D spectra before Fourier transformation, which were composed of $256 \times 256 \times 2048$ points. 2D [^{15}N-^{15}N] (F_1-F_2) slices of the 3D $^{15}N/^{15}N$ separated HSQC-NOESY-TROSY spectrum and its corresponding HSQC-NOESY-HSQC spectrum taken at a ^{1}H chemical shift of $F_3 = 7.92$ ppm are shown in Figures 3A and 3B, respectively. The number beside each peak in Figure 3A is the ratio of the peak intensity in Figure 3A over its corresponding peak intensity in Figure 3B. The improvements in sensitivity and resolution are, overall, the same as those in Figure 2.

Two 2D [^{15}N-^{15}N] (F_1-F_2) slices of the 3D $^{15}N/^{15}N$ separated HSQC-NOESY-TROSY spectrum taken at ^{1}H chemical shifts of $F_3 = 7.66$ ppm and $F_3 = 8.13$ ppm are shown in Figures 4A and 4B, respectively. For those protons with degenerate ^{1}H chemical shift, their NOE cross peaks cannot be observed in a normal 2D [^{1}H-^{1}H]-NOESY spectrum, or a 3D ^{15}N separated NOESY spectrum. However, their cross peaks are clearly seen in Figure 4. It should be noted that the cross peaks on the corners of dashed boxes, corresponding to different coherence transfer paths, respectively, are present on the same plane due to the degeneracy of their proton chemical shifts.

Two 2D spectra ($t_2 = 0$) composed of $54^* \times 2048^*$ points were recorded with 3D TROSY-NOESY-TROSY (Figure 1C) and 3D HSQC-NOESY-TROSY (Figure 1A) pulse sequences. It is shown that the intensity of the former 2D spectrum is only 73% of that of the latter 2D spectrum. This indicates that the replacement of the first HSQC in the 3D HSQC-NOESY-

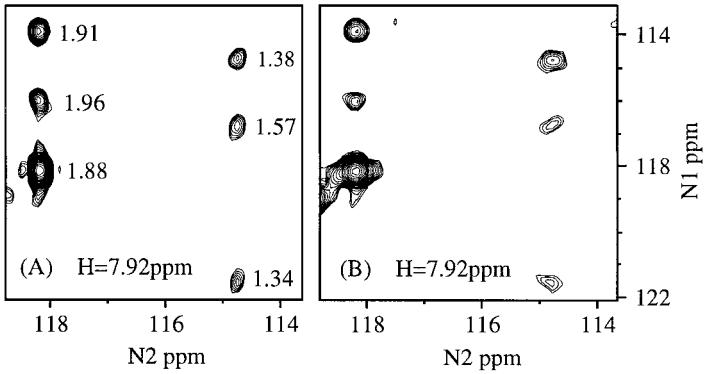

Figure 3. 2D [^{15}N-^{15}N]-slices of the ^{15}N/^{15}N separated 3D HSQC-NOESY-TROSY spectrum (A) and its corresponding HSQC-NOESY-HSQC spectrum (B) of a uniformly 100% ^{15}N and 70% ^{2}H-labeled Trichosanthin sample at 5 °C on a Varian Inova 750 MHz NMR spectrometer, taken at a ^{1}H chemical shift of F_3 = 7.92 ppm. The chemical shifts of the N2 and H_N dimensions in Figure 3A were shifted by 45 Hz compared to those in Figure 3B. The numbers beside the peaks in Figure 3A are the intensity ratios of peaks in Figure 3A and their corresponding peaks in Figure 3B. Figure 3A and Figure 3B have identical lowest contours and a contour factor of 1.2.

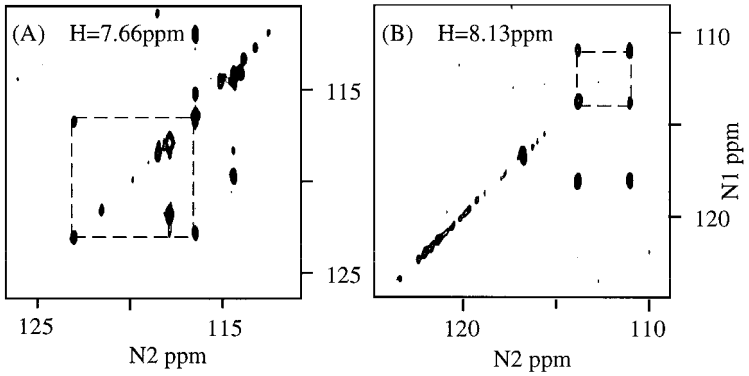

Figure 4. 2D [^{15}N-^{15}N] (F_1-F_2) slices of the 3D ^{15}N/^{15}N separated HSQC-NOESY-TROSY spectrum taken at ^{1}H chemical shifts of F_3 = 7.66 ppm and F_3 = 8.13 ppm, respectively.

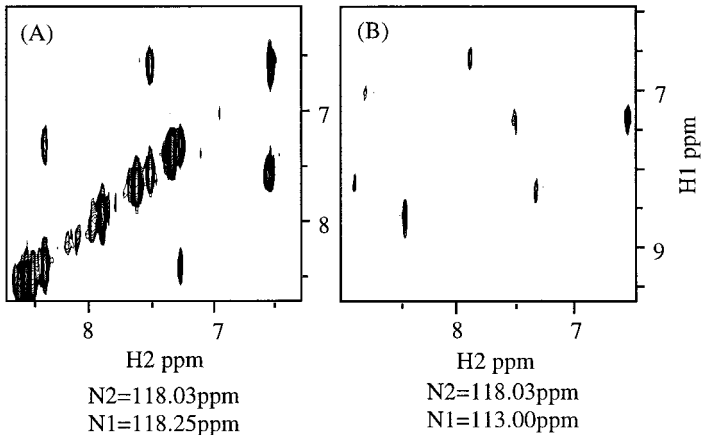

Figure 5. 2D slices of the ^{15}N/^{15}N separated 4D HSQC-NOESY-TROSY spectrum taken from N1 = 118.25 ppm and N2 = 118.03 ppm (A), and N1 = 113.0 ppm and N2 = 118.03 ppm (B) of a uniformly 100% ^{15}N and 70% ^{2}H-labeled Trichosanthin sample at 5 °C on a Varian Inova 750 MHz NMR spectrometer. The chemical shifts of the N2 and H2 dimensions in the two 2D slices were shifted by 45 Hz.

TROSY pulse sequence with TROSY is inappropriate. The reasons are the following: Firstly, the insertion of S^3E into the 3D TROSY-NOESY-TROSY pulse sequence (Figure 1C) increases the signal decay time by 2.7 ms, and reduces signal by a factor of 2 when ignoring the ^{15}N steady-state magnetization. Second, the utilization of the TROSY effect is very limited because the duration of t_1 is limited for practical reasons and the gain from the slowly relaxing component during the t_1 period cannot compensate for the loss of signal. Finally, the first TROSY section in the 3D TROSY-NOESY-TROSY pulse sequence is less effective than the second TROSY section because there are two evolution periods (t_2 and t_3) in the latter section.

In the 4D TROSY-NOESY-TROSY and HSQC-NOESY-TROSY experiments, the TROSY effect is even less significant than that in the 3D experiment, due to shorter evolution times in the t_1, t_2 and t_3 dimensions. It was found in this work that the intensity of the 4D TROSY-NOESY-TROSY (Figure 1D) experiment is less than that of the 4D HSQC-NOESY-TROSY (Figure 1B) experiment, similar to the results for the 3D TROSY-NOESY-TROSY (Figure 1C) and 3D HSQC-NOESY-TROSY (Figure 1A) experiments. Two 3D spectra ($t_3 = 0$) composed of $16^* \times 18^* \times 1024^*$ points with 4D TROSY-NOESY-TROSY (Figure 1D) and 4D HSQC-NOESY-TROSY (Figure 1B) pulse sequences were acquired. It is statistically shown that the intensity of the former 3D spectrum is only 65% of that of the latter 3D spectrum. These results indicate that sensitivity enhancements could be obtained by the replacement of the latter HSQC sections with TROSY in 3D and 4D $^{15}N/^{15}N$ separated HSQC-NOESY-HSQC pulse sequences for the used sample at 5 °C. The sensitivities would be decreased if the first HSQC sections in 3D and 4D $^{15}N/^{15}N$ separated HSQC-NOESY-HSQC pulse sequences are replaced with TROSY sections.

Two 2D spectra ($t_1 = 0$, $t_2 = 0$) with 4D HSQC-NOESY-TROSY (Figure 1B) and 4D HSQC-NOESY-HSQC pulse sequences, composed of $32^* \times 1024^*$ points, were recorded in order to compare the intensities. Although the evolution period of t_3 is shorter, the sensitivity of the former compared to that of the latter is still enhanced by 8%, on average for the 118 well-isolated peaks. Note that if the number of data points in the directly detected dimension is doubled, the sensitivity enhancement would be 18%.

A 4D spectrum, composed of $16^* \times 18^* \times 32^* \times 1024$ points, with spectral widths of $1825 \times 2900 \times 1825 \times 10500$ Hz, was recorded with the 4D HSQC-NOESY-TROSY pulse sequence (Figure 1B). The number of scans for each transient was 4, and the total recording time was 104 h. Cosine square bell window functions were applied to obtain 4D spectra before Fourier transformation. The processed 4D spectrum was composed of $32 \times 32 \times 64 \times 1024$ points. 2D slices of the 4D spectrum taken from N1 = 118.25 ppm (F_1) and N2 = 118.03 ppm (F_3), and N1 = 113.0 ppm and N2 = 118.03 ppm, are shown in Figures 5A and 5B, respectively. NOE cross peaks and diagonal peaks are present in Figure 5A due to the fact that the chemical shifts of N1 and N2 are almost identical. However, only NOE cross peaks are present in Figure 5B due to the fact that the chemical shifts of N1 and N2 are different.

Conclusions

In summary, four 3D and 4D $^{15}N/^{15}N$ separated NOESY experiments are described in this paper. Only the replacements of the latter HSQC sections with TROSY sections are effective, that is, the sensitivity enhancement could be obtained with 3D and 4D $^{15}N/^{15}N$ separated HSQC-NOESY-TROSY pulse sequences. The sensitivities of the two experiments are enhanced by 62% and 8% at 5 °C, respectively, compared to their corresponding 3D and 4D HSQC-NOESY-HSQC experiments. At 25 °C, the 3D $^{15}N/^{15}N$ separated HSQC-NOESY-TROSY experiment is 11% more sensitive than the 3D HSQC-NOESY-HSQC experiment for the Trichosanthin sample used in the present study. The correlation times for Trichosanthin at 5 °C and 25 °C are estimated to be 28 ns and 15 ns by T_1 over T_2 ratio, respectively. It is also noted that the enhancement of sensitivity depends on the molecular mass of the sample used and the lengths of evolution periods in the indirectly and directly detected dimensions. In the present study, linewidths are, on average, decreased by 20% and 18% in the H_N and N2 dimensions, respectively. For a perdeuterated sample, NOEs among amide protons are essential distance constraints, and the 3D and 4D $^{15}N/^{15}N$ separated HSQC-NOESY-TROSY experiments proposed here are important to obtain NOEs for large proteins. Although the 3D and 4D $^{15}N/^{15}N$ separated TROSY-NOESY-TROSY experiments are less sensitive than the 3D and 4D $^{15}N/^{15}N$ separated HSQC-NOESY-TROSY experiments for the testing sample we have used, we believe that the 3D and 4D $^{15}N/^{15}N$ separated TROSY-NOESY-TROSY experi-

ments described here could perform well for a fully deuterated protein with a very small tumbling rate, and with sufficiently long t_1 and t_2 durations for the 3D experiment and long t_1, t_2, and t_3 durations for the 4D experiment.

Acknowledgements

This work is supported by grants from the Research Grant Council of Hong Kong (HKUST6038/98M, 6199/99M and 6208/00M). The Hong Kong Biotechnology Research Institute is acknowledged for the purchase of the 750 MHz NMR spectrometer. We thank Dr. P.C. Shaw for providing the sample used for this study.

References

Delaglio, F., Grzesiek, S., Vuister, G., Zhu, G., Pfeifer, J. and Bax, A. (1995) *J. Biomol. NMR*, **6**, 277–293.

Frenkiel, T., Bauer, C., Carr, M.C., Birdsall, B. and Feeney, J. (1990) *J. Magn. Reson.*, **90**, 420–425.

Ikura, M., Bax, A., Clore, G.M. and Gronenborn, A.M. (1990) *J. Am. Chem. Soc.*, **112**, 9020–9022.

Kay, L.E., Clore, G.M., Bax, A. and Gronenborn, A.M. (1990) *Science*, **249**, 411–414.

Kay, L.E., Keifer, P. and Saarinen, T. (1992) *J. Am. Chem. Soc.*, **114**, 10663–10665.

Meissner, A., Duus, O.J. and Sørensen, O.W. (1997) *J. Biomol. NMR*, **10**, 89–94.

Muhandiram, D.R., Xu, G.Y. and Kay, L.E. (1993) *J. Biomol. NMR*, **3**, 463–470.

Palmer, A.G., Cavanagh, J., Wright, P.E. and Rance, M. (1991) *J. Magn. Reson.*, **93**, 151–170.

Pervushin, K., Riek, R., Wider, G. and Wüthrich, K. (1997) *Proc. Natl. Acad. Sci. USA*, **94**, 12366–12371.

Pervushin, K., Riek, R., Wider, G. and Wüthrich, K. (1998) *J. Am. Chem. Soc.*, **120**, 6394–6400.

Pervushin, K., Wider, G., Riek, R. and Wüthrich, K. (1999) *Proc. Natl. Acad. Sci. USA*, **96**, 9607–9612.

Salzmann, M., Pervushin, K., Wider, G., Senn, H. and Wüthrich, K. (1998) *Proc. Natl. Acad. Sci. USA*, **95**, 13585–13590.

Salzmann, M., Wider, G., Pervushin, K., Senn, H. and Wüthrich, K. (1999a) *J. Am. Chem. Soc.*, **121**, 844–848.

Salzmann, M., Pervushin, K., Wider, G., Senn, H. and Wüthrich, K. (1999b) *J. Biomol. NMR*, **14**, 85–88.

Sørensen, M.D., Meissner, A. and Sørensen, O.W. (1997) *J. Biomol. NMR*, **10**, 181–186.

Torchia, D.A., Sparks, S.W. and Bax, A. (1988) *J. Am. Chem. Soc.*, **110**, 2320–2321.

Venters, R.A., Metzler, W.J., Spicer, L.D., Mueller, L. and Farmer II, B.T. (1995) *J. Am. Chem. Soc.*, **117**, 9592–9595.

Vuister, G.W., Clore, G.M., Gronenborn, A.M., Powers, R., Garrett, D.S., Tschudin, R. and Bax, A. (1993) *J. Magn. Reson.*, **B101**, 210–213.

Weigelt, J. (1998) *J. Am. Chem. Soc.*, **120**, 10778–10779.

Yang, D. and Kay, L.E. (1999) *J. Biomol. NMR*, **13**, 3–10.

Zhu, G., Kong, X.M., Yan. X.Z. and Sze, K.H. (1998) *Angew. Chem. Int. Ed. Engl.*, **37**, 2859–2861.

Zhu, G., Kong, X.M. and Sze, K.H. (1999a) *J. Biomol. NMR*, **13**, 77–81.

Zhu, G., Xia, Y., Sze, K.H. and Yan, X. (1999b) *J. Biomol. NMR*, **14**, 377–381.

Zuiderweg, E.R.P., Petros, A.M., Fesik, S.W. and Olejniczak, E.T. (1991) *J. Am. Chem. Soc.*, **113**, 370–372.